Single-RF Multi-antenna Transmission with Peak Power Constraint

Single-RF Multi-antenna Transmission with Peak Power Constraint

Lin Zhou, Fahd Ahmed Khan, Tharmalingam Ratnarajah, *Senior Member, IEEE,* and Constantinos B. Papadias, *Fellow, IEEE*

***Abstract*—Electronically steerable parasitic array radiator (ESPAR) technology enables the implementation of antenna arrays of a number of elements with a single radio frequency (RF) source. Two approaches to achieve stable transmission using an ESPAR antenna (EA) are to increase the self-resistance of an EA or to transmit signals closely approximating the actual signals that keep the EA stable. Both these approaches did not take into account the impact of limited power on an EA transmission which is a practical constraint on power amplifier design. We propose a new transmission scheme to enable an EA to provide stable multiple antenna functionality taking into account the instantaneous total power requirement. This problem is formulated as a non-convex optimization problem and it is solved analytically by coordinate transformation and geometric analysis. The optimal approximate signals are obtained using root finding and interior-point algorithms. Moreover, it is shown through simulations that our proposed scheme achieves similar symbol error rate (SER) performance to that of the standard multiple antenna transmitter with multiple RF chains under power limited single-user and multi-user transmission scenarios. Furthermore, it is shown that increasing the self-resistance of an EA to achieve stability is highly power inefficient.**

***Index Terms*—Reconfigurable antenna, ESPAR, MIMO transmission, a single RF chain, optimization.**

I. Introduction

Multiple-input multiple-output (MIMO) transmission has been proposed in wireless communication standards including Long Term Evolution (LTE) and LTE advanced (LTE-A) as it provides the benefit of spatial multiplexing and diversity gain [1]. The throughput and the link reliability improve with increasing the number of antennas [2] [3]. A consequence of increasing the number of antennas is that the number of required radio frequency (RF) chains increases linearly with the number of antenna elements, resulting in an increase in the cost and complexity of the device. Moreover, the antenna elements are required to be placed at least half a wavelength apart from each other to minimize the mutual coupling, causing the size of the device to increase [4].

Electronically steerable parasitic array radiator (ESPAR) has been proposed to reduce the cost and the physical size of multiple antenna devices by providing multi-antenna functionality utilizing a single RF chain [5]. The ESPAR antenna (EA) is composed of a compact array with strong coupling among antenna elements. This coupling causes current to flow through the parasitic antenna elements which are without a RF chain. The overall radiation pattern is shaped by controlling the feeding voltage in the RF chain and varying the impedance of parasitic elements [6]. EA offers several advantages. Due to a single RF chain, the cost of the device as well as the circuit energy consumption is reduced and less heat is dissipated [7]. In addition, lower spacing between antenna elements results in a smaller device size [4].

Signal transmission using an EA was initially modeled using the beamspace model [8]. Based on the beamspace model, transmission of a Phase Shift Keying (PSK) modulated signal using an EA with 2 antennas was proposed in [9]. Transmission using an EA with multiple antennas was discussed in [10] and [11]. Proof-of-concept experiments were conducted in an indoor environment with a 2.6-GHz EA prototype and the results were presented in [12]. The beamspace model utilized in these works has several weaknesses [13]. For example, the receiver cannot guarantee orthogonality of the basic beam patterns and arbitrary channel-dependent precoding cannot be realised for an arbitrary antenna array. Therefore, an alternate model based on the currents at the ports of the transmit antenna was introduced in [14], and this model has been further generalized for a single RF chain EA in [4].

Based on this current model, it was shown that the real part of the input impedance of an EA, also labeled as input resistance, must be positive for reliable transmission [15]. Satisfying this condition is essential because

Lin Zhou and Tharmalingam Ratnarajah are with the Institute for Digital Communication (IDCOM), School of Engineering, The University of Edinburgh, Edinburgh, UK, e-mails: l.zhou@ed.ac.uk; t.ratnarajah@ed.ac.uk.

Fahd Ahmed Khan is with the School of Electrical Engineering and Computer Science at National University of Science and Technology, Pakistan. e-mail: fahd.ahmed@seecs.edu.pk.

Constantinos B. Papadias is with Athens Information Technology (AIT), Athens, Greece, e-mail: cpap@ait.gr.

This work was supported by the Seventh Framework Programme for Research of the European Commission under grant number HARP-318489.

a negative input resistance results in a positive reflection coefficient (dB), which implies that the EA is reflecting power back and exhibiting oscillatory/unstable behaviour [16]. In [15], an EA design was proposed which remained stable for an arbitrary precoding scheme. First drawback of this EA design is that it is not generalized for arbitrary modulation and precoding schemes. A new EA needs to be designed if the transmission signal scheme changes [17]. Another drawback of this EA design, which will be discussed later, is that it has high self impedance and thus, very high power consumption. In [17], for arbitrary signal transmission, a different approach was taken and signal approximating the ideal signal in the mean square error (MSE) sense was transmitted using an EA while maintaining stable operation. Benefit of the approach adopted in [17] is that it enables energy efficient transmission for EAs with low self resistance and the EA design does not need to be altered if the transmission precoding scheme is modified.

Unlike the standard multiple antenna system where each RF chain has its own power amplifier, in an EA, all the antennas are fed centrally by a single power amplifier. This makes it more probable that the power amplifier has to operate at very high power [4]. In real world systems, power amplifiers normally support a limited peak power and saturate [18] [19]. This implies that for an EA, it is more likely that the power amplifier will reach maximum power during transmission. At saturation the transmitted signal will distort and result in performance degradation. So, it is necessary to make sure that the power amplifier does not saturate when transmitting using an EA. In existing works, signal transmission schemes were proposed for an EA without taking into account the saturation of a power amplifier. In this work, we propose a new transmission signal design for an EA such which ensures stable operation and does not saturate the power amplifier. Considering a constraint on the saturation/peak power, is also useful in the context of wireless sensor networks, internet of things and device-to-device communication which have limited power available for communication [4]. This makes EA utilizing our proposed transmission scheme, a promising candidate for such technologies as it enables multiple antenna functionality with smaller device sizes and at a lower cost.

Following a similar approach to [17], signals closely approximating the ideal signals, in the MSE sense, are transmitted. Approximate signals are generated taking into account the saturation power of the amplifier. Specifically, in order to obtain the approximate signal, an optimization problem is formulated to minimize the MSE between the ideal and approximate signals ensuring that the power amplifier does not saturate and the EA maintains stable operation. To the authors best knowledge, this approach is new and has not been considered in literature previously. In deriving the approximate signals, it is assumed that the EA transmitter has perfect channel state information[1]. The underlying optimization problem has a quadratic objective function and two non-convex quadratic constraints. This new problem is not convex and challenging to solve the strong duality conditions used in [17] and [20] cannot be applied to this problem[2]. Instead coordinate transform and geometric methods are applied to find the best approximate signals. By using coordinate transform and geometric method, semi-definite relaxation was avoided and the actual problem was solved instead of an approximate problem. After solving and simplifying the optimization problem, the approximate transmission signals is shown that these approximate signals can be easily obtained using root finding and interior point algorithms.

The performance of our proposed algorithm is analyzed using EAs which were designed in [14] and [22]. The symbol error ratio (SER) performance of our proposed algorithm is compared with the SER performance of a standard multiple antenna transmitter in various communication scenarios. Specifically, we consider both single-user and multi-user scenarios. For the single-user scenario, as an example, we analyze the SER performance of the proposed algorithm for Alamouti coded transmission and maximum ratio transmission. For the multi-user case, the performance of the proposed algorithm is shown for channel inversion (CI) and regularized channel inversion (RCI) precoder. Our results show that a system employing an EA transmitter and using our proposed algorithm gives similar perfor-

[1]Channel estimation using an ESPAR antenna is challenging and must be taken into account. In this work, we have considered perfect channel state information which provides a benchmark for performance. One of the issues which arises in ESPAR based systems is that the active antenna elements must work all the time. For standard multiple antenna transmission, one antenna element maybe activated in a time slot and its channel maybe estimated. For ESPAR based transmitter this is not possible. One of the feasible solutions for channel estimation is to use orthogonal training sequences for estimation, in order to estimate the channel from each of the antenna elements. So, a challenge in this case is to design an orthogonal training signal to estimate the channel. Due to space limitation, channel estimation related issues for EA will be considered in a future work.

[2]The underlying optimization problem maybe solved using SDR. However, we have used a method based on coordinate transformation and geometric methods to solve as it always guaranteed the optimal solution with lower complexity. The worst case complexity of the proposed algorithm is $\mathcal{O}\left(16M^2 - 4M + 8\log\frac{1}{\xi}\right)$, where M is the total number of transmitting antenna elements. The SDR problem can be solved with a complexity of $\mathcal{O}\left((2M)^{4.5}\log\frac{1}{\xi}\right)$ by counting the arithmetic operations of a specific interior-point method in [21]. Thus, complexity of SDR based approach is much higher compared to our proposed method.

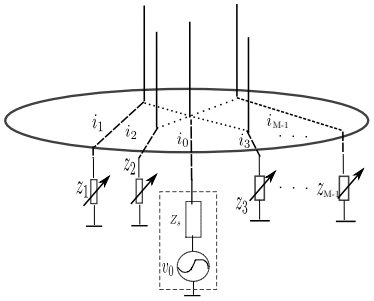

Fig. 1: Model of a circular EA

mance as the system with a standard multiple antenna transmitter. Moreover, in [15], stable EA transmission was achieved by increasing the self-resistance of the active element. Our results show that if the EA has a large self-resistance, as in [15], the performance is significantly degraded. Due to a large self-resistance, large amount of power is dissipated at the self-resistance and only limited power is actually transmitted. This results in significantly degraded performance and in order to reduce the SER, the peak power needs to be increased substantially which renders the EA with a large self-resistance highly power inefficient regardless of its improved stability. This shows that it is not an energy efficient approach to improve the stability of an EA by increasing its self-resistance.

The rest of the paper is organized as follows. The EA transmitter is described in section II and the power model is explained in section II-B. The corresponding problem is formulated and discussed in Section III, followed by application in Section IV. Finally, the main results are concluded in the concluding Section V.

II. System Model for ESPAR MIMO

A. ESPAR Antenna Transmitter

Fig. 1 shows a block diagram of an EA consisting of a single active element with a RF unit and $M-1$ parasitic elements without any RF units. Z_m denotes the tunable impedance at the m-th parasitic element. The current in the active element, i_0, is varied by varying the value of the voltage feeding. As the antenna elements are closely spaced, when feeding the active element, the currents are induced on the parasitics elements. The current in the m-th parastic element, i_m, can be varied by adjusting the variable impedance, z_m. Where as in traditional multiple antenna transmitters with multiple RF chains, the currents are driven by the RF voltage supply of each antenna element through fixed impedances [23].

An EA, is specified by a mutual coupling matrix, $Z \in \mathbb{C}^{M\times M}$, which quantifies the mutual coupling between antenna elements and depends on the antenna geometry [24]. A mutual coupling matrix can be expressed as

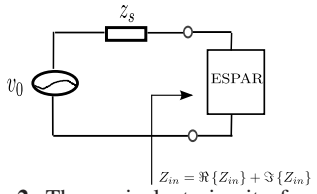

Fig. 2: The equivalent circuit of an EA

$$\mathbf{Z} = \begin{bmatrix} Z_{00} & Z_{01} & \cdots & Z_{0(M-1)} \\ Z_{10} & Z_{11} & \cdots & Z_{1(M-1)} \\ \vdots & \vdots & \ddots & \vdots \\ Z_{(M-1)0} & Z_{(M-1)2} & \cdots & Z_{(M-1)(M-1)} \end{bmatrix}. \tag{1}$$

where Z_{ij} denotes the mutual coupling impedance between the i-th and j-th elements in an EA.

Based on circuit theory, the current flowing through the antenna element of an EA can be mathematically expressed as

$$\mathbf{i} = (\mathbf{Z} + \mathbf{Z}_L)^{-1} \mathbf{v}. \tag{2}$$

where $\mathbf{i} = [i_0, i_1, \ldots, i_{M-1}]^T$ is the vector of currents at the antenna elements, $\mathbf{v} = [v_0, 0, 0, \ldots, 0]^T$ denotes the voltage vector, $\mathbf{Z}_L = \text{diag}\,(z_s, z_1, z_2, \ldots, z_{M-1})$ is the impedance matrix composed of z_s at the active element and the tunable loads of the parasitic elements at its diagonal entries and T denotes the transpose operator. When current $\mathbf{i}$ flows through the antenna elements, the input impedance of an EA, as depicted in Fig. 2, is given by [15]

$$Z_{in} = Z_{00} + \frac{\sum_{m=1}^{M-1} Z_{0m} i_m}{i_0}. \tag{3}$$

Note that Z_{in} is a function of the MC values Z_{ij} and the currents i_m depend on the value of the voltage feeding v_0 and the tunable loads z_m.

B. Power Consideration Using an EA

Using the equivalent circuit model of an EA as shown in Fig. 2, the power delivered to an EA can be mathematically expressed as

$$\begin{aligned} P_E = i_0^2 \Re\{Z_{in}\} &= \left|\frac{v_0}{z_s + Z_{in}}\right|^2 \Re\{Z_{in}\} \\ &= \left|\frac{v_0}{z_s + Z_{in}}\right|^2 \left\{ R_0 + \Re\left\{ \frac{\sum_{m=1}^{M-1} Z_{0m} i_m}{i_0} \right\} \right\}, \end{aligned} \tag{4}$$

where R_0 is self resistance of the active element, $\Re\{Z_{in}\}$ and $\Im\{Z_{in}\}$ denote its resistive and reactive components of the input impedance, respectively. In order to guarantee stable transmission, the input power to an EA should be positive, which implies the $\Re\{Z_{in}\}$ should be positive. If $\Re\{Z_{in}\}$ is not positive, it means that the EA is reflecting power back and exhibiting oscillatory/unstable behavior [16].

It is desirable to have a reasonable value of self resistance, not too large and neither too small. The larger the value of R_0, its more likely that the input impedance will remain positive and the EA will remain stable for most transmission signals. However, it will consume a large amount of power as can be noted from (4). Small values of R_0 will more likely result the input impedance to become negative for more transmission signals. This implies that, larger the value of R_0, the EA will remain stable for majority of signals and lower the value of R_0, the EA will exhibit unstable behaviour for a large set of signals. A more detailed discussion on this is given in [17].

Let w_{2m+1} and w_{2m+2} from the vector $\mathbf{i}$ denote the real part and the imaginary part of i_m. Representing the current values in (3) in terms of w_{2m+1} and w_{2m+2} and substituting it in (4), the input power to the active element can be simplified as

$$P_E = \left(w_1^2 + w_2^2\right) \Re \left\{ Z_{00} + \frac{\sum_{m=1}^{M-1} Z_{0m} i_m}{i_0} \right\}. \quad (5)$$

Following the method proposed in Appendix A in [17], the input power to the antenna element can be reformulated in the real domain as shown in the following proposition.

Proposition 1 *The power supplied to an EA from the active element is given as*

$$P_E = \mathbf{w}^T \mathbf{A} \mathbf{w}, \quad (6)$$

where $\mathbf{w} = [w_1, w_2, w_3, w_4, \ldots, w_{2M-1}, w_{2M}]^T$ *and its elements* w_{2m+1} *and* w_{2m+2} *denote the real part and the imaginary part of* i_m*, respectively. A is given as* (7)*. where* R_m *and* X_m *denote the real part and the imaginary part of the mutual coupling from the active element to the* m*-th parasitic element,* Z_{0m}*.*

Using (3) and after some mathematical manipulations, the voltage feeding and load values can be calculated from $\mathbf{w}$ as

$$v_0 = 2 \sum_{j=0}^{M-1} Z_{0j} \left(w_{2j} + j w_{2j+1}\right), \quad (8a)$$

$$z_m = -\frac{\sum_{j=0}^{M-1} Z_{mj} \left(w_{2j} + j w_{2j+1}\right)}{\left(w_{2m} + j w_{2m+1}\right)}, \quad (8b)$$

$$m = 1, 2, \ldots, M-1. \quad (8c)$$

C. Impedance Matching

For maximum power transfer, impedance matching is necessary. The generator/source impedance needs to be matched to the overall input impedance of the EA. In [15], a dynamic impedance matching circuit is proposed to compensate the impedance mismatch between the source and input impedance of the EA. The total power supplied by source in the active element is

$$P_S = i_0^2 \Re \left\{ z_s + Z_{in} \right\} = 2 P_E. \quad (9)$$

D. Point-to-point System Model

Consider a link consisting of a transmitter having an array of M antennas and a receiver having N_r antennas. The corresponding signal model is

$$\mathbf{y} = \mathbf{H}\mathbf{i} + \mathbf{n}, \quad (10)$$

where $\mathbf{y}$ is the received signal at the receiver, $\mathbf{H} \in \mathbb{C}^{N_r \times M}$ is the channel matrix, $\mathbf{i}$ is the vector of currents flowing through the transmit antennas, and $\mathbf{n} \in \mathbb{C}^{N_r \times 1}$ denotes the noise vector. The noise is assumed to be additive white Gaussian noise (AWGN) with zero mean and unit variance.

III. Algorithm for Signal Transmission under Limited Power

For signal transmission, the currents at the antenna element need to be varied based on input data symbols. As discussed previously, this variation in current is achieved by varying the loads at the parasitic elements and the voltage feeding at the active element. In some cases, for a certain transmission signal, it is possible that the the voltage feeding and the tunable loads take values which lead to a negative input resistance, causing an EA to exhibit unstable behaviour. For transmission of such signals, it was proposed to transmit signals closely approximating the ideal signal and which keep the EA stable by making sure that the input impedance remains positive for all signals [17]. However, in [17], no limit on the power of an EA was assumed. So, in that scheme it is possible that the power required by the EA is sufficiently high to saturate the power amplifier. This saturation of a power amplifier can be avoided by generating signals for which the peak power remains below the saturation power of the power amplifier.

The problem to obtain the values of the voltage and the loadings can be formulated as an optimization problem to minimize the MSE between the currents corresponding to the ideal and approximate transmission signals, and is given as (11). where $\hat{\mathbf{i}}$ denotes the desired current vector corresponding to ideal signal required to be transmitted by the EA, P_S^{min} is the minimal transmitted power which ensure the stable work of an EA and P_S^{max} is the saturation power of the power amplifier. The objective of this optimization problem is to find the voltage feeding v_0 and the loads $z_1, z_2, \ldots, z_{M-1}$ to minimize MSE between the ideal and approximate signal. Constraint (11b) is to guarantee that the input

$$\mathbf{A} = \begin{bmatrix} R_0 & 0 & \frac{R_1}{2} & -\frac{X_1}{2} & \dots & \frac{R_{M-1}}{2} & -\frac{X_{M-1}}{2} \\ 0 & R_0 & \frac{X_1}{2} & \frac{R_1}{2} & \dots & \frac{X_{M-1}}{2} & \frac{R_{M-1}}{2} \\ \frac{R_1}{2} & \frac{X_1}{2} & 0 & 0 & \dots & 0 & 0 \\ -\frac{X_1}{2} & \frac{R_1}{2} & 0 & 0 & \dots & 0 & 0 \\ \vdots & \vdots & \vdots & \vdots & \ddots & \vdots & \vdots \\ \frac{R_{M-1}}{2} & \frac{X_{M-1}}{2} & 0 & 0 & \dots & 0 & 0 \\ -\frac{X_{M-1}}{2} & \frac{R_{M-1}}{2} & 0 & 0 & \dots & 0 & 0 \end{bmatrix} \tag{7}$$

$$\min_{v_0, \mathbf{Z}_L} \quad \left\| \hat{\mathbf{i}} - (\mathbf{Z} + \mathrm{diag}(z_s, z_1, z_2, \dots, z_{M-1}))^{-1} [v_0, 0, \dots, 0] \right\|_2 \tag{11a}$$

$$\text{st.} \quad P_S = 2 \left| \frac{v_0}{z_s + Z_{in}} \right|^2 \Re\{Z_{in}\} \geq P_S^{min} \tag{11b}$$

$$P_S = 2 \left| \frac{v_0}{z_s + Z_{in}} \right|^2 \Re\{Z_{in}\} \leq P_S^{max} \tag{11c}$$

resistance is positive and that the EA does not exhibit unstable behaviour. Constraint (11c) guarantees that the peak power remains below the saturation power of the power amplifier.

A. Problem Reformulation

Let $P_{min} = \frac{P_S^{min}}{2}$ and $P_{max} = \frac{P_S^{max}}{2}$, the optimization problem can be reformulated and represented in terms of real and imaginary part of current in the antenna elements as

$$\min_{\mathbf{w}} \quad \|\mathbf{w} - \hat{\mathbf{w}}\|^2, \tag{12a}$$

$$\text{st.} \quad \mathbf{w}^T \mathbf{A} \mathbf{w} > P_{min}, \tag{12b}$$

$$\mathbf{w}^T \mathbf{A} \mathbf{w} \leq P_{max}. \tag{12c}$$

where $\hat{\mathbf{w}} = [\hat{w}_1, \hat{w}_2, \hat{w}_3, \hat{w}_4, \dots, \hat{w}_{2M-1}, \hat{w}_{2M}]^T$, where $\hat{w}_{2m+1}$ and $\hat{w}_{2m+2}$ denote the real part and the imaginary part of $\hat{i}_m$, respectively.

The problem in (12) has a quadratic objective function and two quadratic constraints and the number of optimization variables is $2M$. Following a similar approach as in Appendix C in [17], it can be shown that $\mathbf{A}$ is an indefinite matrix and its eigenvalues are

$$\begin{cases} \lambda_1 = \lambda_2 = R_0 - \sqrt{R_0^2 + \sum_{m=1}^{M-1} (R_m^2 + X_m^2)} \\ \lambda_{2M-1} = \lambda_{2M} = R_0 + \sqrt{R_0^2 + \sum_{m=1}^{M-1} (R_m^2 + X_m^2)} \\ \lambda_n = 0 \quad \text{for } n = 3, 4, \dots, 2M-2 \end{cases} \tag{13}$$

where $\lambda_1, \lambda_2, \dots, \lambda_{2M-1}, \lambda_{2M}$ denotes the eigenvalues of the matrix $\mathbf{A}$ in ascending order. It can be noted that λ_1, λ_2 are negative, and λ_3, λ_4 are positive. Thus, this implies that the optimization problem in (12) is non-convex.

Due to the non-convex nature of the constraint set, the strong duality employed in [17] and [20], cannot be applied to this problem. Instead we use coordinate transform and geometric method to solve the optimization problem.

As $\mathbf{A}$ is a real symmetric matrix, it can be diagonalized as $\mathbf{A} = \mathbf{Q}\mathbf{\Lambda}_A\mathbf{Q}^T$, where $\mathbf{\Lambda}_A = [\lambda_1, \lambda_2, \dots, \lambda_{2M-1}, \lambda_{2M}]$ is a real diagonal matrix consisting of eigenvalues of $\mathbf{A}$ and the columns of the real orthogonal matrix $\mathbf{Q}$ are corresponding eigenvectors. By applying a linear transformation on vectors $\mathbf{w}$ and $\hat{\mathbf{w}}$, as $\mathbf{e} = \mathbf{Q}^\mathbf{T}\mathbf{w} = [e_1, e_2 \dots, e_{2M-1}, e_{2M}]^T$ and $\mathbf{g} = \mathbf{Q}^T\hat{\mathbf{w}} = [g_1, g_2, \dots, g_{2M-1}, g_{2M}]^T$, the problem in (13) is simplified.

Proposition 2 *The optimization problem in* (12) *can be reformulated as*

$$\min_{\bar{\mathbf{e}}} \quad \|\bar{\mathbf{e}} - \bar{\mathbf{g}}\|^2, \tag{14a}$$

$$\textit{st.} \quad \bar{\mathbf{e}}^T \,\mathrm{diag}\,(\lambda_1, \lambda_2, \lambda_{2M-1}, \lambda_{2M})\, \bar{\mathbf{e}} > P_{min}, \tag{14b}$$

$$\bar{\mathbf{e}}^T \,\mathrm{diag}\,(\lambda_1, \lambda_2, \lambda_{2M-1}, \lambda_{2M})\, \bar{\mathbf{e}} \leq P_{max}, \tag{14c}$$

where $\bar{\mathbf{e}} = [e_1, e_2, e_{2M-1}, e_{2M}]^T$ *and* $\bar{\mathbf{g}} = [g_1, g_2, g_{2M-1}, g_{2M}]^T$. *The minimum is obtained when* $e_m = g_m$, for $m = 3, 4, \dots, 2M-2$.

Proof: The proof is provided in Appendix A. ■

It can be noted that the optimization problem in (14) is more simplified and has 4 optimization variables instead of $2M$.

,

B. Solution of the Optimization Problem

The optimization problem in (14) can be further simplified using coordinate transformation. Representing the elements of $\bar{\mathbf{e}}$ and $\bar{\mathbf{g}}$ into polar coordinate system as $e_1 = r_a \cos\theta_a$, $e_2 = r_a \sin\theta_a$, $e_{2M-1} = r_b \cos\theta_b$, $e_{2M} = r_b \sin\theta_b$, $g_1 = r_c \cos\theta_c$, $g_2 = r_c \sin\theta_c$, $g_{2M-1} = r_d \cos\theta_d$, $g_{2M} = r_d \sin\theta_d$, respectively, where $r_a = \sqrt{e_1^2 + e_2^2}$, $\theta_a = \arctan\left(\frac{e_2}{e_1}\right)$, $r_b = \sqrt{s_{2M-1}^2 + e_{2M}^2}$, $\theta_b = \arctan\left(\frac{e_{2M}}{e_{2M-1}}\right)$, $r_c = \sqrt{g_1^2 + g_2^2}$, $\theta_c = \arctan\left(\frac{g_2}{g_1}\right)$, $r_d = \sqrt{g_{2M-1}^2 + g_{2M}^2}$,

and $\theta_d = \arctan\left(\frac{g_{2M}}{g_{2M-1}}\right)$. Using this coordinate transformation, the problem can be further reformulated as shown in the following proposition.

Proposition 3 *By replacing Cartesian coordinate with polar system in* (14)*, the objective function* $\|\bar{\mathbf{e}} - \bar{\mathbf{g}}\|^2$ *achieves its minimal value when* $\theta_a = \theta_c$ *and* $\theta_b = \theta_d$*. Therefore, the problem in* (14) *can be further simplified as*

$$\min_{r_a, r_b} \quad r_a^2 + r_b^2 - 2r_a r_b - 2r_c r_d + r_c^2 + r_d^2, \tag{15a}$$

$$\textit{st.} \quad \lambda_1 r_a^2 + \lambda_{2M-1} r_b^2 \geq P_{min}, \tag{15b}$$

$$\lambda_1 r_a^2 + \lambda_{2M-1} r_b^2 \leq P_{max}. \tag{15c}$$

Proof: The proof is provided in Appendix B. ■

It can be noted from Proposition 3 that the optimal value of θ_a and θ_b are obtained. Therefore, the number of optimization variables has been reduce to two and it is required to obtain values of r_a and r_b which minimizes (15a) under the constraints (15b) and (15c). The constraint set can be written as (16).

$\lambda_1 r_a^2 + \lambda_{2M-1} r_b^2 = P_{min}$ and $\lambda_1 r_a^2 + \lambda_{2M-1} r_b^2 = P_{max}$ are two hyperbolas with same asymptotes and different focus points. The constraint set is the area between the hyperbola $\lambda_1 r_a^2 + \lambda_{2M-1} r_b^2 = P_{min}$ and hyperbola $\lambda_1 r_a^2 + \lambda_{2M-1} r_b^2 = P_{max}$, which is not a convex set.

Viewing (15) in light of the constraint set $\mathbb{S}_1$, the optimization problem is to find a point $(r_a, r_b) \in \mathbb{S}_1$ which is closest to point (r_c, r_d). Thus, the optimization problem in (15) can be restated to find the optimal point $(r_a, r_b) \in \mathbb{S}_1$ which has minimum Euclidean distance to the point (r_c, r_d) as (17).

This problem can be subdivided into three sub-optimization problems according to the position of the point $\mathbf{r}_g$.

1) Case 1: $\mathbf{r}_g \in \mathbb{S}_1$*:* If $\mathbf{r}_g \in \mathbb{S}_1$, then $\textbf{dist}(\mathbf{r}_g, \mathbb{S}_1) = 0$. In this case, $\mathbf{r}_e = \mathbf{r}_g$.

2) Case 2: $\left\{\mathbf{r}_g = (r_c, r_d) \mid \lambda_1 r_c^2 + \lambda_{2M-1} r_d^2 \leq P_{min}\right\}$*:* This scenario will occur when the ideal signal might cause the EA to become unstable. In this case, $\mathbf{r}_e$ will be a point on the hyperbola which is nearest to $\mathbf{r}_g$. This problem can be reformulated as a second order cone program (SOCP) as given in the following proposition.

Proposition 4 *For case 2, the optimization problem in* (15) *can be reformulated as a convex second-order cone programming (SOCP)*

$$\min_{\mathbf{r}_e} \quad \|\mathbf{r}_e - \mathbf{r}_g\|_2^2, \tag{18a}$$

$$\textit{st.} \quad \left\| \frac{\sqrt{2}\frac{r_a}{\left(1/\sqrt{-\lambda_1}\right)} + \frac{r_b}{\left(1/\sqrt{\lambda_{2M-1}}\right)}}{\sqrt{P_{min}}} \right\| \tag{18b}$$

$$\leq \sqrt{2}\frac{r_b}{\left(1/\sqrt{\lambda_{2M-1}}\right)} + \frac{r_a}{\left(1/\sqrt{-\lambda_1}\right)}. \tag{18c}$$

Proof: The proof is provided in Appendix C. ■

The problem in (15) is a standard SOCP program, which can be solved using an interior point algorithm [20].

3) Case 3: $\left\{\mathbf{r}_g = (r_c, r_d) \mid \lambda_1 r_c^2 + \lambda_{2M-1} r_d^2 > P_{max}\right\}$*:* This scenario will occur when the ideal signal is such that the peak power constraint is violated. In this case, $\mathbf{r}_e$ will be a point on the hyperbola which is nearest to $\mathbf{r}_g$. This optimization problem can be expressed

$$\textbf{dist}(\mathbf{r}_g, \mathbb{S}_1) = \inf\left\{\|\mathbf{r}_g - \mathbf{r}_e\| \mid \lambda_1 r_a^2 + \lambda_{2M-1} r_b^2 = P_{max}, \right\}. \tag{19}$$

Proposition 5 *The optimal* $\mathbf{r}_e$ *for the problem in* (19) *is* $\left(\frac{r_c}{1+\lambda_1 t}, \frac{r_d}{1+\lambda_{2M-1} t}\right)$*, where* t *is the unique root of the function* $G(t) = \lambda_1\left(\frac{r_c}{1+\lambda_1 t}\right)^2 + \lambda_{2M-1}\left(\frac{r_d}{1+\lambda_{2M-1} t}\right)^2 - P_{max} = 0$ *in the interval* $\left\{t | -\frac{1}{\lambda_{2M-1}} \leq t \leq -\frac{1}{\lambda_1}\right\}$.

Proof: The proof is provided in Appendix D. ■

In order to obtain the optimal value of $\mathbf{r}_e$ mentioned in Proposition 5, a root is required. Any root finding algorithm can be used. However, in our algorithm, we use the method which combines the bisection and Newton's method [25] [26]. Firstly, the bisection method is utilised to reduce the search area. Then Newton's method is applied to find the root. The steps are outlined in Algorithm 1.

Once the optimization problem is solved, the optimal approximate signals can be obtained for the EA. The main steps for calculation of the optimal approximate signals are outlined in Algorithm 2.

C. Complexity Analysis of Proposed Algorithm

From Algorithm 2, the solution of the optimization problem is solved from Step 4 to Step 12. If the SDR approach is adopted, it will also apply from (12) and the number of optimization variables is $2M$. Below we calculate the complexity of our proposed algorithm. In the proposed algorithm, during the signal transmission, the steps from step 1 to step 3 can be calculated once, and can be used for the subsequent signal transmissions. Only step 4 to step 12 require to be calculated for every transmitted signal.

Step 4: Step 4 involves a matrix multiplication operation, thus it requires $2n^2 - n = 8M^2 - 2M$ floating point (flop) operations [27] [28].

Step 5 to Step 7: Step 5 to step 7 involves 6 operations of scalar multiplication, 2 operations of scalar division and 2 operations of inverse tangent based on scalars.

Step 8: Step 8 involves a SOCP and the number of optimization variables has been reduce to two. As the worst-case complexity on the order is $\mathcal{O}\left(n^3 \log\frac{1}{\xi}\right)$ for

$$\mathbb{S}_1 = \left\{ \mathbf{r}_e = (r_a, r_b) \mid \lambda_1 r_a^2 + \lambda_{2M-1} r_b^2 \geq P_{min}, \lambda_1 r_a^2 + \lambda_{2M-1} r_b^2 \leq P_{max} \right\} \tag{16}$$

$$\textbf{dist}\left(\mathbf{r}_g, \mathbb{S}_1\right) = \inf\left\{ \|\mathbf{r}_g - \mathbf{r}_e\| \mid \mathbf{r}_e = (r_a, r_b) \in \mathbb{S}_1,\ \mathbf{r}_g = (r_c, r_d) \in \mathbb{R}^2 \right\} \tag{17}$$

Algorithm 1 Finding the projection of $\mathbf{r}_g$ onto the hyperbola $\mathbb{S}_1$

Input: $\mathbf{r}_g$, $\lambda_1^{(A)}$, $\lambda_{2M-1}^{(A)}$, P_{max};
Output: $\mathbf{r}_e$;
Step 1: Choose the inflection points as the initial data point in canonical coordinates, and calculate inflection point t_0 and the corresponding $G(t_0)$.
Step 2: If $G(t_0) < 0$, then pick the interval $\mathbb{D} = \left(-\frac{1}{\lambda_{2M-1}}, t_0\right]$.
  for $j = 1 : N_{div}$
    $t_0^{old} = t_0^{new}$; $t_0^{new} = \left(-\frac{1}{\lambda_1}\right)^2 - \frac{\left(-t_0^{old} + \left(-\frac{1}{\lambda_1}\right)\right)}{2^j}$;
    if $G\left(t_0^{new}\right) < 0$ break; end;
  end;
for $iter = 1 : N$
    $t_0^{old} = t_0^{new}$;
    if $G\left(t_0^{old}\right) > 0$ break; end;
    if $\left|\frac{G\left(t_0^{old}\right)}{G'\left(t_0^{old}\right)}\right| < \xi$ break; end
    $t_0^{new} = t_0^{old} - \frac{G\left(t_0^{old}\right)}{G'\left(t_0^{old}\right)}$;
  end
Step 3: If $G(t_0) > 0$ then pick the initial interval $\mathbb{D} = \left[t_0, -\frac{1}{\lambda_1}\right)$.
  for $j = 1 : N_{div}$
    $t_0^{old} = t_0^{new}$; $t_0^{new} = -\left(-\frac{1}{\lambda_{2M-1}}\right)^2 - \frac{\left(t_0^{old} - \left(-\frac{1}{\lambda_{2M-1}}\right)\right)}{2^j}$;
    if $G\left(t_0^{new}\right) > 0$ break; end;
  end;
  for $iter = 1 : N$
    $t_0^{old} = t_0^{new}$;
    if $G\left(t_0^{old}\right) < 0$ break; end;
    if $\left|\frac{G\left(t_0^{old}\right)}{G'\left(t_0^{old}\right)}\right| < \xi$ break; end
    $t_0^{new} = t_0^{old} - \frac{G\left(t_0^{old}\right)}{G'\left(t_0^{old}\right)}$;
  end
Step 4: Substitute t_0^{new} to $\left(\frac{r_c}{1+\lambda_1 t}, \frac{r_d}{1+\lambda_{2M-1} t}\right)$ to obtain $\mathbf{r}_e$.

Algorithm 2 Finding optimal transmission signals and corresponding values of voltage feeding and load for an EA

Input: Required ideal currents vector $\hat{\mathbf{i}}$
Output: EA-P loads and voltage feeding for $\hat{\mathbf{i}}$,
Step 1: if $\hat{\mathbf{i}} \in \mathbb{I}_{P\xi}$ {Goto Step 6. } else {Goto Step 2.}
Step 2: Obtain $\hat{\mathbf{w}}$ by separating real and imaginary parts of $\hat{\mathbf{i}}$. Calculate $\mathbf{A}$.
Step 3: Calculate λ_1, λ_{2M-1}, and $\mathbf{Q}$ from the eigenvalue decomposition of $\mathbf{A}$.
Step 4: Calculate $\mathbf{g}$ by $\mathbf{g} = \mathbf{Q}^T \hat{\mathbf{w}}$.
Step 5: Calculate r_c, r_d, θ_c and θ_d by $r_c = \sqrt{g_1^2 + g_2^2}$, $\theta_c = \arctan\left(\frac{g_2}{g_1}\right)$, $r_d = \sqrt{g_{2M-1}^2 + g_{2M}^2}$, and $\theta_d = \arctan\left(\frac{g_{2M}}{g_{2M-1}}\right)$.
Step 6: Calculate e_m, for $m = 3, 4, \ldots, 2M_t - 2$, θ_a and θ_b by $e_m = g_m$, for $m = 3, 4, \ldots, 2M_t - 2$, $\theta_a = \theta_c$ and $\theta_b = \theta_d$, respectively.
Step 7: Calculate $\lambda_1 r_c^2 + \lambda_{2M-1} r_d^2$
  if $\lambda_1 r_c^2 + \lambda_{2M-1} r_d^2 < P_{min}$ Goto Step 8;
  else if $\lambda_1 r_c^2 + \lambda_{2M-1} r_d^2 > P_{max}$ Goto Step 9;
  else $\mathbf{r}_e = \mathbf{r}_g$; Goto Step 10;
  end;
Step 8: Calculate r_a, r_b by Proposition 4.
Step 9: Calculate r_a, r_b by Algorithm 1.
Step 10: Using Proposition 3, $\theta_a = \theta_c$ and $\theta_b = \theta_d$.
Step 11: Calculate the elements of $\mathbf{s}$ by $e_1 = r_a \cos\theta_a$, $e_2 = r_a \sin\theta_a$, $e_{2M-1} = r_b \cos\theta_b$, $e_{2M} = r_b \sin\theta_b$, $e_m = g_m$, for $m = 3, 4, \ldots, 2M$.
Step 12: Calculate $\mathbf{w}$ from $\mathbf{w} = \mathbf{Q}\mathbf{e}$.
Step 13: Calculate the corresponding loads $z_1, z_2, \ldots, z_{M-1}$ and feeding v_0 as (8).

SOCPs [29] and $n = 2$, the complexity for this step is $\mathcal{O}\left(8 \log \frac{1}{\xi}\right)$. It is also noted the worst-case complexity on the order of $\mathcal{O}\left(n^{4.5} \log \frac{1}{\xi}\right)$ for SDPs [29] and the SOCP is more efficient than the SDR in terms of the execution time [29] [30].

Step 9: Step 9 requires calculating the root. The number of optimization variables is one. The complexity of the root finding algorithm is $\mathcal{O}\left(log \frac{1}{\xi}\right)$ [25] [26].

Step 10 to Step 11: Step 10 involves operations of scalar assignment, 4 operations of scalar multiplication, 2 scalar sine operations and 2 scalar cosine operations.

Step 12: Step 12 involves matrix operations and it requires $2n^2 - n = 8M^2 - 2M$ flops.

Adding the complexity of each step, the worst case complexity of the proposed algorithm is $\mathcal{O}\left(16M^2 - 4M + \log \frac{1}{\xi}\right)$.

IV. Applications and Numerical Analysis

In this section, using numerical simulations, we analyse the performance of an EA using our proposed Algorithm 2 in various communication scenarios.

A. Single-user Scenario

Consider a point-to-point link consisting of a transmitter having an array of M antennas and a receiver

having N_r antennas. The corresponding signal model is given by (7). In order to radiate the signal, the currents at the antenna element need to be varied based on the transmission signal [14], [31], [32]. Without loss of generality, as we focus on the transmitter scheme with an EA, in our simulations, we assume that the receiver has a single antenna element. The channel is assumed to be Rayleigh faded.

Diversity gain is one of the main advantages of multiple antennas which results in significant performance improvement. There are different approaches to achieve transmit diversity gain depending on the CSI availability at the transmitter [2].

1) Transmitter without CSI: In this case, the diversity gain can be achieved by using Alamouti scheme, which extracts transmit diversity without transmitter CSI. For a two element EA, given a transmission symbol vector $[s_0, s_1]^T$, the ideal currents are$\hat{\mathbf{i}} = \sqrt{\frac{P_T}{M}} \begin{bmatrix} s_0 & -s_1^* \\ s_1 & s_0^* \end{bmatrix}$, where P_T is transmitted signal power from the EA. The corresponding power consumption for these two symbol periods is

$$\begin{aligned} P_E^{(1)} &= i_1^2 R_{in} = \frac{P_T}{M} |s_0|^2 \left(R_0 + \Re \left(\frac{Z_{01} s_1}{s_0} \right) \right), \\ P_E^{(2)} &= i_1^2 R_{in} = \frac{P_T}{M} |s_1|^2 \left(R_0 + \Re \left(\frac{Z_{01} s_0^*}{-s_1^*} \right) \right). \end{aligned} \tag{20}$$

The supported signal vector set $[s_0, s_1]^T$, which can be exactly transmitted using the Alamouti code by a EA, is (21).

It can be noted from (20) and (21) that whether a signal can be supported depends on the MC matrix and also the transmission signals which depend on the modulation scheme employed. For example, consider N-PSK modulation scheme. Assume that the signal at the $(m+1)$-th element is denoted as $s_m = \exp(j\phi_m)$, where $\phi_m = \frac{2\pi n_m}{N}, n_m \in \{0, 1, ..., (N-1)\}$ is the phase of the signal at the $(m+1)$-th antenna element and N is the order of the PSK signal constellation [9]. In this case, the input power for the combination of N-PSK signals can be expressed as (22). The corresponding input power for two signal periods is

$$\begin{aligned} P_E^{(1)} &= i_1^2 R_{in} = \frac{P_T}{M} (R_0) + \frac{P_T}{M} R_1 \left(\cos \frac{2\pi (n_m - n_0)}{N} \right) \\ &\quad - \frac{P_T}{M} R_1 \left(X_1 \sin \frac{2\pi (n_m - n_0)}{N} \right), \\ P_E^{(2)} &= i_1^2 R_{in} = \frac{P_T}{M} (R_0) - \frac{P_T}{M} \left(R_1 \cos \frac{2\pi (n_m - n_0)}{N} \right) \\ &\quad + \frac{P_T}{M} \left(X_1 \sin \frac{2\pi (n_m - n_0)}{N} \right). \end{aligned} \tag{23}$$

Therefore, in order to transmit different N-PSK signals for each antenna element, the MC matrix of the EA is required to satisfy (24).

It can be noted that the input power varies with R_0, R_1 and X_1 (defined by the MC matrix), the required transmitted power and the phases of transmitted signals. When the transmitter uses BPSK, then the MC matrix is required to satisfy that $P_{min} < P_T \frac{R_0 \pm R_1}{M} < P_{max}$. Note that the power of an EA increases linearly with R_0. For a transmitter which supports limited power, either due to finite battery or to avoid saturation of the power amplifier, it is undesirable to have a high R_0. However, as shown in [17], a higher value of R_0 increases the stability of an EA.

Numerical Simulation: The SER performance of the system where the transmitter employs Alamouti code is shown in Fig 3. P_T is transmitted signal power from the EA. Noise is assumed to be addictive white Gaussian noise (AWGN) with zero mean and unit variance, therefore, it is equivalent to the transmission SNR. The modulation scheme is 16-QAM and the SER performance of an EA using our proposed algorithm is compared to the SER performance of a standard multiple antenna transmitter. The EA using our proposed algorithm is denoted by EA-P and the standard multiple antenna transmitter is denoted by SMA. For the simulation, we select three practical 2-element EAs with MC matries, $\mathbf{Z}^{(1)}$, $\mathbf{Z}^{(2)}$, and $\mathbf{Z}^{(3)}$, and three MCMs for 2-element ESPAR in the IE3D antenna software are

$$\mathbf{Z}^{(1)} = \begin{bmatrix} 45.12 - j16.60 & 42.39 - j29.51 \\ 42.39 - j29.51 & 21.12 - j29.64 \end{bmatrix},$$

$$\mathbf{Z}^{(2)} = \begin{bmatrix} 52.81 - j11.09 & 40.27 - j20.75 \\ 40.27 - j20.75 & 52.81 - j11.09 \end{bmatrix},$$

$$\mathbf{Z}^{(3)} = \begin{bmatrix} 465.4 - j659.5 & -24.06 + j34.93 \\ -24.06 + j34.93 & 21.12 - j157.2 \end{bmatrix},$$

These EAs have been designed using IE3D antenna design software in [15] [22] [3].

The values of self-resistance for $\mathbf{Z}^{(1)}$, $\mathbf{Z}^{(2)}$ and $\mathbf{Z}^{(3)}$ are 45.12, 52.81 and 465.4, respectively. The EA with $\mathbf{Z}^{(3)}$ has the largest self-resistance designed to overcome the stability problem for an EA transmitter [15]. Without loss of generality $P_{min} = 0$ and $P_{max} = 100, 150$.

[3]The ESPAR antenna with MCM $\mathbf{Z}^{(1)}$ and $\mathbf{Z}^{(3)}$ were designed in [15]. The authors, in [15] designed an EA with MCM, $\mathbf{Z}^{(3)}$, which has a large self resistance. It was shown that this EA remains stable for arbitrary signal transmission. So this is a benefit of using $\mathbf{Z}^{(3)}$ that it remains stable for most signals. The authors in [15] also showed that it achieves similar performance to a SMA system. However, the EA with MCM $\mathbf{Z}^{(3)}$ has a large self impedance which implies that it consumes a large amount of power. The ESPAR antenna with MC $\mathbf{Z}^{(2)}$ was obtained by IE3D as in [22] and the proposed circuit design was presented in [33]. IE3D from Mentor Graphics is a full-wave, method-of-moments electromagnetic design and verification platform that delivers the modeling accuracy for the combined needs of high-frequency circuit design and signal integrity engineers across multiple design domains.

$$\mathbb{S}_{P\xi} = \left\{ [s_0, s_1] \middle| P_{min} < P_E^{(1)} \leq P_{max}, P_{min} < P_E^{(2)} \leq P_{max} \right\} \tag{21}$$

$$\begin{aligned} P_E = i_1^2 R_{in} &= \frac{P_T}{M} |s_0|^2 \Re \left(Z_{00} + \sum_{m=1}^{M-1} Z_{0m} \exp\left(j\left(\phi_m - \phi_0\right)\right) \right) \\ &= \frac{P_T}{M} \left(R_0 + \sum_{m=1}^{M-1} \left(R_m \cos \frac{2\pi\left(n_m - n_0\right)}{N} - X_m \sin \frac{2\pi\left(n_m - n_0\right)}{N} \right) \right) \end{aligned} \tag{22}$$

$$\mathbf{Z} \in \left\{ \mathbf{Z} \middle| \frac{P_{min}}{P_T} < \frac{1}{M} \left(R_0 \pm \left(R_1 \cos\left(\phi_1 - \phi_0\right) + X_1 \sin\left(\phi_1 - \phi_0\right) \right) \right) < \frac{P_{max}}{P_T} \right\} \tag{24}$$

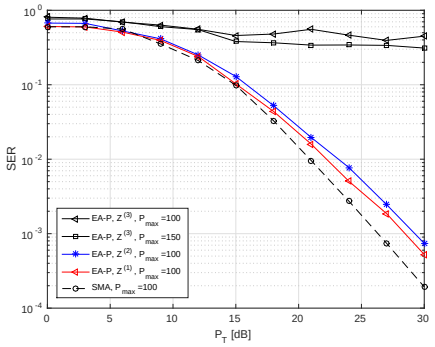

Fig. 3: SER performance comparison of the ESPAR transmitter and the standard multiple antenna transmitter employing Almouti scheme with 16-QAM modulation.

For the EAs with $\mathbf{Z}^{(1)}$ and $\mathbf{Z}^{(2)}$, the SER for the EA transmission is slightly higher compared to the SMA system. This can be expected because, unlike the SMA, the EA is transmitting approximate signals instead of the ideal signals. The EA with $\mathbf{Z}^{(3)}$ was designed to overcome the stability problem for an EA transmitter in [15]. However, considering the maximal power requirement of EA, it consumes large power as the self-resistance at the active element is large. Due to this large self-resistance, in order to meet the power constraint the symbol transmission power is reduced which results in significantly degraded performance. This shows that achieving stability by increasing the self-resistance is highly power inefficient approach.

2) Transmitter with CSI: When the transmitter has CSI, transmit diversity can be achieved by employing maximal ratio transmission (MRT). Assuming that symbol s is to be transmitted, the symbols are precoded and mapped to the antenna currents. Let $\mathbf{h} = [h_0, h_1, \ldots, h_{M-1}]^H \in \mathbb{C}^{M\times 1}$ and h_m denotes the channel from the $(m+1)$-th element of EA transmitter to the signal antenna receiver. h_m is a Rayleigh random variable. The ideal port current at the transmitter is $\hat{\mathbf{i}} = \sqrt{P_T}\frac{\mathbf{h}}{\|\mathbf{h}\|}s$. For N-PSK modulation, the corresponding power consumption at the active element can be obtained as

$$\begin{aligned} P_E &= P_T \left(\frac{h_0 s}{\|\mathbf{h}\|} \right)^2 \Re \left(Z_{00} + \frac{\sum_{m=1}^{M-1} Z_{0m} h_j}{h_0} \right) \\ &= P_T \left(\frac{h_0}{\|\mathbf{h}\|} \right)^2 \left(R_0 + \Re \left(\frac{\sum_{m=1}^{M-1} Z_{0m} h_j}{h_0} \right) \right). \end{aligned} \tag{25}$$

It can be noted that the input power varies with channel and the MC matrix, and that it is independent of the data symbols. This implies that, for the EA, in the case of a block fading channel, in which the channel is constant over a block of symbols, the antenna only needs to be preprocessed once in the beginning of the block.

Numerical Simulation: Considering MRT scheme, the SER performances are compared for EAs with different number of elements and spacings in Fig. 4 and Fig. 5. In Fig. 4, it can be observed that the SER performance of EAs with MCM $\mathbf{Z}_1$ and $\mathbf{Z}_2$ is similar to that of the standard multiple antenna transmitter especially at low SNRs. Similar to Fig. 3 as P_T increases, the power consumed by the antenna approaches P_{max} and an error floor occurs. However, again, with the maximal power constraint, the EA with $\mathbf{Z}^{(3)}$ is unable to achieve SER close to the SER of a standard multiple antenna system.

As shown in Fig. 5, the mutual coupling matrices for different number of antenna elements are obtained using the induced electromotive force method (IEFM) for different antenna spacing [34]. The SER performance for two different antenna spacing $d = \frac{\lambda}{4}$ for linear EAs are shown in the Fig. 5. It can be observed from this figure that the SER performance varies with the number of antenna elements and the antenna spacing. Increasing the number of the elements or reducing antenna spacing reduces the SER.

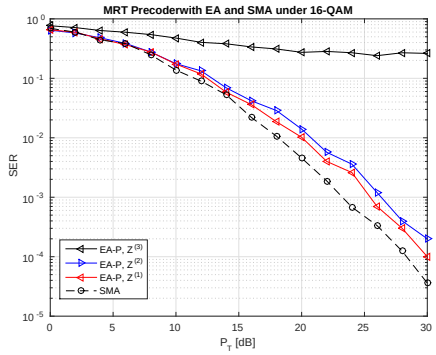

Fig. 4: SER performance comparison of the EA transmitter and the standard multiple antenna transmitter employing MRT scheme with 16-QAM modulation.

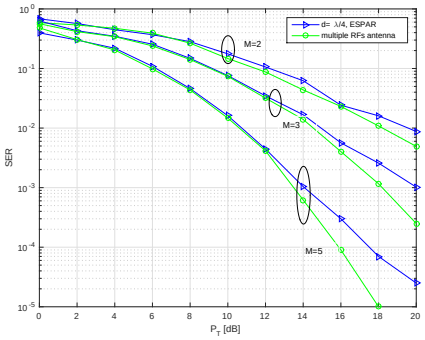

Fig. 5: SER performance comparison of the EA transmitter and the standard multiple antenna transmitter with different number of antenna elements employing MRT schemen.

B. Multi-user Scenario

Next, we investigate the application of the proposed antenna to MU-MIMO systems. We consider the downlink multi-user scenario where the base station communicates with several single-antenna users. Let us assume the transmit symbol vector $\mathbf{u} = [u_1, u_2, \ldots, u_K]^T$, in which, u_k denotes the transmit symbol to the k-th user. The desired transmitted current vector $\mathbf{i}$ can be expressed as

$$\mathbf{i} = \mathbf{F}\mathbf{u}. \tag{26}$$

At the base station, the symbol vector for user is precoded and $\mathbf{F}$ is the precoding matrix.

We consider channel inversion (CI), and regularized channel inversion (RCI) as precoding schemes for downlink transmissions. Denoting the precoding matrix by $\mathbf{F} \in \mathbb{S}^{M\times K}$, we have that

$$\mathbf{F} = \begin{cases} \mathbf{H}^H \left(\mathbf{H}\mathbf{H}^H\right)^{-1} & CI, \\ \mathbf{H}^H \left(\mathbf{H}\mathbf{H}^H + \sigma^2 \mathbf{I}_{M-1}\right)^{-1} & RCI. \end{cases} \tag{27}$$

Then the transmit current vector can be expressed as $\hat{\mathbf{i}} = \sqrt{\frac{P_t}{R_{ref}}}\mathbf{F}\mathbf{s}$, and the corresponding power consumption for an EA is

$$P_E^{(1)} = i_1^2 R_{in} = P_T \left|(\mathbf{F}\mathbf{s})^{(0)}\right|^2 \Re\left(Z_{00} + \frac{\sum_{m=1}^{M-1} Z_{0m}(\mathbf{F}\mathbf{s})}{(\mathbf{F}\mathbf{s})^{(0)}}\right). \tag{28}$$

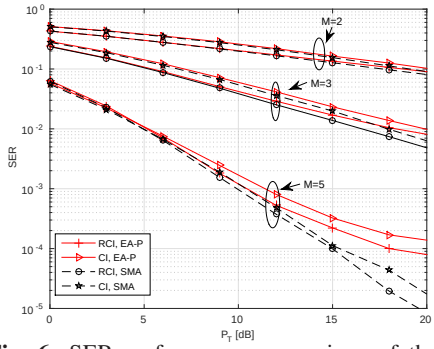

Fig. 6: SER performance comparison of the EA transmitter and the standard multiple antenna transmitter employing RCI and CI schemes with QPSK modulation.

Numerical Simulation: In the simulation, EA is employed at the base station and serve two single-antenna users. The MCM is calculated by induced electromotive force method (IEFM) [35] for thin half-wavelength electrical dipoles EA. The antenna spacing is assumed to $d = \lambda/4$, where λ denotes the wavelength at 2.6 GHz. The modulation scheme in the simulations is QPSK. The SER performances are compared for EAs with different number of antenna elements in Fig 6 for CI and RCI algorithms. Again, the SER performance of the EA transmitter is similar to that of the standard multiple antenna transmitter at low P_T. At high P_T, the performance saturates due to limited maximum power. Moreover, RCI gives better performance compared to CI as it takes into account the noise power.

V. Conclusion

An EA is unable to transmit all types of signals as some signals lead to unstable behaviour of an EA. Considering limited power availability, we propose a new algorithm to achieve stable signal transmission using an EA. It is shown that the system employing the proposed transmission scheme gives similar performance to that of a standard multiple antenna system, especially at low SNRs. In addition, it is shown that improving the stability by increasing theself-resistance increases the power consumption proportionally and thus, for practical systems with limited power, it is highly power inefficient and infeasible. These results are verified through extensive simulation results of an EA system in various communication scenarios.

APPENDIX A
PROOF OF PROPOSITION 2

Proof: As $\mathbf{A}$ is a real symmetric matrix and it can be diagonalized as $\mathbf{A} = \mathbf{Q}\mathbf{\Lambda}_A\mathbf{Q}^T$, where $\mathbf{\Lambda}_A$ is a real diagonal matrix whose elements are eigenvalues of $\mathbf{A}$. The columns of the orthogonal matrix $\mathbf{Q}$ are the corresponding eigenvectors. Let $\mathbf{e} = \mathbf{Q^T w}$, $\mathbf{g} = \mathbf{Q}^T\hat{\mathbf{w}}$. By substituting them into (12a), the objective function of this optimization problem can be written as

$$\begin{aligned}\|\mathbf{w}-\hat{\mathbf{w}}\|^2 &= (\mathbf{Q}(\mathbf{e}-\mathbf{g}))^T(\mathbf{Q}(\mathbf{e}-\mathbf{g}))\\ &= (\mathbf{e}-\mathbf{g})^T(\mathbf{e}-\mathbf{g}) = \|\mathbf{e}-\mathbf{g}\|^2.\end{aligned} \tag{29}$$

Similarly, the left side of the constraints (12b) and (12c) can be written as

$$\mathbf{w}^T\mathbf{A}\mathbf{w} = \mathbf{e}^T\mathbf{\Lambda_A}\mathbf{e}. \tag{30}$$

Thus, the optimization problem can be reformulated as

$$\min_{\mathbf{e}} \quad \|\mathbf{e}-\mathbf{g}\|_2^2, \tag{31a}$$

$$\text{st.} \quad \mathbf{e}^T\mathbf{\Lambda_A}\mathbf{e} \geq P_{min}, \tag{31b}$$

$$\mathbf{e}^T\mathbf{\Lambda_A}\mathbf{e} \leq P_{max}. \tag{31c}$$

By substituting the elements of $\mathbf{g}$ and $\mathbf{e}$ into (31), the objective function can be further reformulated as

$$\begin{aligned}\|\mathbf{e}-\mathbf{g}\|_2^2 = &\sum_{m=1}^{2}(e_m-g_m)^2\\ &+\sum_{m=3}^{2M-2}(e_m-g_m)^2+\sum_{m=2M-1}^{2M}(e_m-g_m)^2,\end{aligned} \tag{32}$$

and the corresponding constraints are

$$\begin{aligned}&\lambda_1\left(e_1^2+e_2^2\right)+\lambda_{2M-1}\left(e_{2M-1}^2+e_{2M}^2\right)\geq P_{min},\\ &\lambda_1\left(e_1^2+e_2^2\right)+\lambda_{2M-1}\left(e_{2M-1}^2+e_{2M}^2\right)\leq P_{max}.\end{aligned} \tag{33}$$

Note that the elements $e_m,\ m=3,4,\ldots,2M$ are not in the constraints. Therefore, in order to minimize (32), $e_m = g_m,$ for $m = 3,4,\ldots,2M$. By setting $\bar{\mathbf{e}} = [e_1,e_2,e_{2M-1},e_{2M}]^T$, $\bar{\mathbf{g}} = [g_1,g_2,g_{2M-1},g_{2M}]^T$ and $\mathbf{\Lambda}_1 = diag\left(\lambda_1,\lambda_1,\lambda_{2M-1},\lambda_{2M-1}\right)$, (31) can be further simplified as

$$\min_{\mathbf{e}} \quad \|\mathbf{e}-\bar{\mathbf{g}}\|^2, \tag{34a}$$

$$\text{st.} \quad \mathbf{e}^T\,\mathrm{diag}\left(\lambda_1,\lambda_2,\lambda_{2M-1},\lambda_{2M}\right)\mathbf{e} > P_{min}, \tag{34b}$$

$$\mathbf{e}^T\,\mathrm{diag}\left(\lambda_1,\lambda_2,\lambda_{2M-1},\lambda_{2M}\right)\mathbf{e} \leq P_{max}. \tag{34c}$$

(34) can be expressed in matrix form as in (14). ■

APPENDIX B
PROOF OF PROPOSITION 3

Proof: By substituting the polar coordinate forms into (14), its constraints can be rewritten as

$$\begin{aligned}&\lambda_1 r_a^2+\lambda_{2M-1}r_b^2\geq P_{min},\\ &\lambda_1 r_a^2+\lambda_{2M-1}r_b^2\leq P_{max}.\end{aligned} \tag{35}$$

As $r_a \geq 0$, $r_b \geq 0$, $\lambda_1 < 0$, $\lambda_{2M-1} > 0$, the objective function (14a) can be expressed as

$$\begin{aligned}&\|\bar{\mathbf{e}}-\bar{\mathbf{g}}\|^2 = \sum_{m=1}^{2}(e_m-g_m)^2+\sum_{m=2M-1}^{2M}(e_m-g_m)^2\\ =&r_a^2+r_b^2-2r_ar_c\left(\cos\theta_a\cos\theta_c-\sin\theta_a\sin\theta_c\right)\\ &+r_c^2+r_d^2-2r_br_c\left(\cos\theta_b\cos\theta_d-\sin\theta_b\sin\theta_d\right)\\ =&r_a^2+r_b^2-2r_ar_c\cos\left(\theta_a-\theta_c\right)-2r_br_c\cos\left(\theta_b-\theta_d\right)\\ &+r_c^2+r_d^2.\end{aligned} \tag{36}$$

As there is no constraint on θ_a and θ_b, the objective function achieves its minimal value when when $\theta_a = \theta_c$ and $\theta_b = \theta_d$. Thus, the optimal point of θ_a and θ_b are θ_c and θ_d, respectively. By substituting the optimal points, (36) can be expressed as

$$\begin{aligned}\|\bar{\mathbf{e}}-\bar{\mathbf{g}}\|^2 &\geq r_a^2+r_b^2-2r_ar_c-2r_br_c+r_c^2+r_d^2\\ &= (r_a-r_c)^2+(r_b-r_d)^2.\end{aligned} \tag{37}$$

(37) and (35) give the objective function and constraints of (3), respectively. ■

APPENDIX C
PROOF OF PROPOSITION 4

Proof: The problem can be expressed as

$$\min_{\mathbf{s}} \quad \|\mathbf{r}_e-\mathbf{r}_g\|_2^2, \tag{38a}$$

$$\text{st.} \quad \lambda_1 r_a^2+\lambda_1 r_b^2 \geq P_{min}, \tag{38b}$$

where $\mathbf{r}_e = [r_a, r_b]$ and $\mathbf{r}_g = [r_c, r_d]$ As the left side of the constrait (38b) can be written as

$$\lambda_1 r_a^2+\lambda_{2M-1}r_b^2 = \left(\frac{r_b^2}{\left(1/\sqrt{\lambda_{2M-1}}\right)^2}-\frac{r_a^2}{\left(1/\sqrt{-\lambda_1}\right)^2}\right)\geq P_{min}, \tag{39}$$

therefore, it can be reformulated as

$$\begin{aligned}&2\frac{r_b^2}{\left(1/\sqrt{\lambda_{2M-1}}\right)^2}+\frac{r_a^2}{\left(1/\sqrt{-\lambda_1}\right)^2}\\ &\geq 2\frac{r_a^2}{\left(1/\sqrt{-\lambda_1}\right)^2}+\frac{r_b^2}{\left(1/\sqrt{\lambda_{2M-1}}\right)^2}+P_{min}.\end{aligned} \tag{40}$$

Then

$$\left\|\begin{matrix}\sqrt{2}\frac{r_a}{\left(1/\sqrt{-\lambda_1}\right)}+\frac{r_b}{\left(1/\sqrt{\lambda_{2M-1}}\right)}\\ \sqrt{P_{min}}\end{matrix}\right\| \leq \sqrt{2}\frac{r_b}{\left(1/\sqrt{\lambda_{2M-1}}\right)}+\frac{r_a}{\left(1/\sqrt{-\lambda_1}\right)}. \tag{41}$$

■

APPENDIX D
PROOF OF PROPOSITION 5

Proof: When setting $r_a = \sec(\theta)$, and $r_b = \tan(\theta)$, the distance from $\mathbf{r}_g$ and the hyperbola can be expressed as

$$F(\theta) = |\mathbf{r}_g-\mathbf{r}_e|^2. \tag{42}$$

As $F(\theta)$ is a non-negative, periodic, and differentiable function, it must have a global minimum occurring at an angle for which the first-order derivative is zero,

$$F^{'}(\theta) = 2(\mathbf{r}_g - \mathbf{r}_e)\,\mathbf{r}_g^{'}. \tag{43}$$

For the derivative to be zero, the vectors $\mathbf{r}_g - \mathbf{r}_e$ and $\mathbf{r}_g^{'}$ must be perpendicular. The vector $\mathbf{r}_g^{'}$ is tangent to the ellipse at $\mathbf{r}_g$. This implies that the vector from $\mathbf{r}_g$ to the closest ellipse point $\mathbf{r}_e$ is normal to the curve at $\mathbf{r}_g$. Using the implicit form of the ellipse, namely, $\lambda_1 r_a^2 + \lambda_{2M-1} r_b^2 = P_{max}$, half of its gradient is a normal vector to the ellipse at (r_a, r_b), so $(r_c, r_d) - (r_a, r_b) = t(\lambda_1 r_a, \lambda_2 r_b)$ for some scalar t, or

$$r_c = r_a(1+\lambda_1 t),\ r_d = r_b(1+\lambda_{2M-1} t). \tag{44}$$

As all signals are transmitted through the antenna elements, and $r_c > 0$, $r_d > 0$, we have

$$r_a = \frac{r_c}{1+\lambda_1 t}, r_b = \frac{r_d}{1+\lambda_{2M-1} t}. \tag{45}$$

In order to describe the constraint area, we introduce a auxiliary function $G = \lambda_1 r_a^2 + \lambda_{2M-1} r_b^2 - P_{max}$. By substitute (45) into it to obtain

$$G(t) = \lambda_1 \left(\frac{r_c}{1+\lambda_1 t}\right)^2 + \lambda_{2M-1}\left(\frac{r_d}{1+\lambda_{2M-1} t}\right)^2 - P_{max}. \tag{46}$$

We know that the closest point in the first quadrant requires $1+\lambda_{2M-1} t \geq 0$ and $1+\lambda_1 t \geq 0$, which implies $t \geq -\frac{1}{\lambda_{2M-1}}$ and $t \leq -\frac{1}{\lambda_1}$.

The first-order derivative of $G(t)$ are

$$G^{'}(t) = -\frac{2\lambda_1^2 r_c^2}{(1+\lambda_1 t)^3} - \frac{2\lambda_{2M-1}^2 r_d^2}{(1+\lambda_{2M-1} t)^3} < 0. \tag{47}$$

For $t \geq -\frac{1}{\lambda_{2M-1}}$ and $t \leq -\frac{1}{\lambda_1}$, we have the conditions $G^{'}(t) < 0$. Also observe that

$$\begin{aligned} \lim_{t \to \left(-\frac{1}{\lambda_1}\right)^+} G^{'}(t) &= -\infty, \\ \lim_{t \to \left(-\frac{1}{\lambda_{2M-1}}\right)^-} G^{'}(t) &= +\infty. \end{aligned} \tag{48}$$

These two expressions are one-sided limits where t approaches $-\frac{1}{\lambda_{2M-1}}$ through values larger than $-\frac{1}{\lambda_1}$. We have shown that $F(t)$ is a strictly decreasing function for $t \in (-\frac{1}{\lambda_{2M-1}}, -\frac{1}{\lambda_1})$ that is initially positive, then becomes negative. Consequently it has a unique root on the specified domain. ■

REFERENCES

[1] S. Sesia, M. Baker, and I. Toufik, *LTE-the UMTS long term evolution: from theory to practice*. John Wiley & Sons, 2011.

[2] D. Tse and P. Viswanath, *Fundamentals of wireless communication*. Cambridge university press, 2005.

[3] E. Biglieri, MIMO *wireless communications*. Cambridge University Press, 2007.

[4] M. A. Sedaghat, V. I. Barousis, C. Papadias *et al.*, "Load modulated arrays: a low-complexity antenna," *IEEE Communications Magazine*, vol. 54, no. 3, pp. 46–52, 2016.

[5] T. Ohira and K. Iigusa, "Electronically steerable parasitic array radiator antenna," *Electronics and Communications in Japan (Part II: Electronics)*, vol. 87, no. 10, pp. 25–45, 2004.

[6] R. Harrington, "Reactively controlled directive arrays," *IEEE Trans. Antennas Propag.*, vol. 26, no. 3, pp. 390–395, May 1978.

[7] L. Zhou, T. Ratnarajah, J. Xue, and F. Khan, "Energy efficient cloud radio access network with a single rf antenna," in *2016 IEEE International Conference on Communications (ICC)*, May 2016, pp. 1–6.

[8] A. Kalis, A. Kanatas, and C. Papadias, "A novel approach to MIMO transmission using a single RF front end," *IEEE J. Sel. Areas Commun.*, vol. 26, no. 6, pp. 972–980, 2008.

[9] O. Alrabadi, C. Papadias, A. Kalis, and R. Prasad, "A universal encoding scheme for MIMO transmission using a single active element for PSK modulation schemes," *IEEE Trans. Wireless Commun.*, vol. 8, no. 10, pp. 5133–5142, 2009.

[10] V. Barousis, A. Kanatas, and A. Kalis, "Beamspace-domain analysis of single-RF front-end MIMO systems," *IEEE Trans. Veh. Technol.*, vol. 60, no. 3, pp. 1195–1199, 2011.

[11] O. Alrabadi, J. Perruisseau-Carrier, and A. Kalis, "MIMO transmission using a single RF source: Theory and antenna design," *IEEE Trans. Antennas Propag.*, vol. 60, no. 2, pp. 654–664, 2012.

[12] O. N. Alrabadi, C. Divarathne, P. Tragas, A. Kalis, N. Marchetti, C. B. Papadias, and R. Prasad, "Spatial multiplexing with a single radio: Proof-of-concept experiments in an indoor environment with a 2.6-ghz prototype," *Communications Letters, IEEE*, vol. 15, no. 2, pp. 178–180, 2011.

[13] C. B. Papadias, "An emerging technology: load-modulated arrays for small and large scale mimo systems," in *Presentation given in the Smart Antennas Workshop, Stanford, USA*, 2014.

[14] V. Barousis, C. Papadias, and R. Muller, "A new signal model for MIMO communication with compact parasitic arrays," in *Communications, Control and Signal Processing (ISCCSP), 2014 6th International Symposium on*, 2014, pp. 109–113.

[15] V. Barousis and C. Papadias, "Arbitrary precoding with single-fed parasitic arrays: Closed-form expressions and design guidelines," *IEEE Wireless Communications Lett.*, vol. PP, no. 99, pp. 1–4, 2014.

[16] D. M. Pozar, *Microwave engineering*. Wiley, 2012.

[17] L. Zhou, F. A. Khan, T. Ratnarajah, and C. B. Papadias, "Achieving arbitrary signals transmission using a single radio frequency chain," *IEEE Trans. Commun.*, vol. 63, no. 12, pp. 4865–4878, 2015.

[18] A. C. Cirik, L. Zhou, and T. Ratnarajah, "Linear transceiver design with per-antenna power constraints in full-duplex multi-user mimo systems," *IEEE Wireless Communications Letters*, vol. 5, no. 4, pp. 412–415, 2016.

[19] W. Yu and T. Lan, "Transmitter optimization for the multi-antenna downlink with per-antenna power constraints," *IEEE Transactions on Signal Processing*, vol. 55, no. 6, pp. 2646–2660, 2007.

[20] S. Boyd and L. Vandenberghe, *Convex optimization*. Cambridge university press, 2009.

[21] Z.-Q. Luo, W.-K. Ma, A.-C. So, Y. Ye, and S. Zhang, "Semidefinite relaxation of quadratic optimization problems," *IEEE Signal Process. Mag.*, vol. 27, no. 3, pp. 20–34, May 2010.

[22] B. Han, V. Barousis, C. Papadias, A. Kalis, and R. Prasad, "MIMO over ESPAR with 16-QAM modulation," *IEEE Wireless Communications Lett.*, vol. 2, no. 6, pp. 687–690, December 2013.

[23] M. T. Ivrlac and J. A. Nossek, "Toward a circuit theory of communication," *IEEE Trans. Circuits Syst.*, vol. 57, no. 7, pp. 1663–1683, 2010.

[24] C. A. Balanis, *Antenna theory: analysis and design*. John Wiley & Sons, 2012.

[25] D. Eberly, "Distance from a point to an ellipse, an ellipsoid, or a hyperellipsoid."

[26] D. H. Eberly, *3D game engine design: a practical approach to real-time computer graphics*. CRC Press, 2006.

[27] R. Hunger, *Floating point operations in matrix-vector calculus*. Munich University of Technology, Inst. for Circuit Theory and Signal Processing Munich, 2005.

[28] G. H. Golub and C. F. Van Loan, *Matrix computations*. JHU Press, 2012, vol. 3.

[29] E. Dall'Anese and G. B. Giannakis, "Sparsity-leveraging reconfiguration of smart distribution systems," *IEEE Transactions on Power Delivery*, vol. 29, no. 3, pp. 1417–1426, 2014.

[30] Q. Shi, W. Xu, T. H. Chang, Y. Wang, and E. Song, "Joint beamforming and power splitting for miso interference channel with swipt: An socp relaxation and decentralized algorithm,"

IEEE Transactions on Signal Processing, vol. 62, no. 23, pp. 6194–6208, 2014.
[31] G. Alexandropoulos, V. Barousis, and C. Papadias, "Precoding for multiuser mimo systems with single-fed parasitic antenna arrays," in *Global Communications Conference (GLOBECOM), 2014 IEEE*, Dec 2014, pp. 3897–3902.
[32] D. F. Kelley and W. L. Stutzman, "Array antenna pattern modeling methods that include mutual coupling effects," *IEEE Trans. Antennas Propag.*, vol. 41, no. 12, pp. 1625–1632, 1993.
[33] B. Han, V. I. Barousis, A. Kalis, C. B. Papadias, A. G. Kanatas, and R. Prasad, "A single rf mimo loading network for high-order modulation schemes," *International Journal of Antennas and Propagation*, vol. 2014, 2014.
[34] W. L. Stutzman and W. A. Davis, *Antenna theory*. Wiley Online Library, 1998.
[35] L. Petit, L. Dussopt, and J.-M. Laheurte, "MEMS-switched parasitic-antenna array for radiation pattern diversity," *IEEE Trans. Antennas Propag.*, vol. 54, no. 9, pp. 2624–2631, 2006.

Lin Zhou received the dual B.Sc. degrees in Communication Engineering & Computer Science, and the M.Sc. degree in Electronics and Information Engineering from Huazhong University of Science and Technology, Wuhan, China, in 2004 and 2007 respectively. She is currently working toward her PhD at The University of Edinburgh, Edinburgh, U.K., from 2013. From 2004 to 2007, she had been with Wuhan National Laboratory for Optoelectronics, China, working on the implementation of Beyond 3G wireless communication systems as an R&D engineer. From 2007 to 2012, she has been working as an integrated circuit (IC) design engineer on computer science and telecommunication in O2micro and Fiberhome, respectively. Her research interests include design and modeling of compact MIMO transceivers, CRANs and energy efficient wireless networks.

Fahd Ahmed Khan received the B.Sc. degree in electrical engineering from the National University of Science and Technology, Pakistan, the masters degree in communications engineering from Chalmers University of Technology, Gothenburg, Sweden, and the Ph.D. degree in electrical engineering from King Abdullah University of Science and Technology (KAUST), Thuwal, Saudi Arabia, in 2007, 2009, and 2013, respectively. He was a Research Fellow with the Institute for Digital Communications, University of Edinburgh, U.K., from November 2013 to November 2014. Currently, he is working as an Assistant Professor at the School of Electrical Engineering and Computer Science in National University of Science and Technology, Pakistan. His research interests include performance analysis of multiple antenna communication, cooperative relaying networks and cognitive radio networks. He was the recipient of the Academic Excellence Award from KAUST, in 2010 and 2011, respectively, and was also the recipient of the best poster award at IEEE DySPAN 2012.

Tharmalingam Ratnarajah (A96-M05-SM05) is currently with the Institute for Digital Communications, University of Edinburgh, Edinburgh, UK, as a Professor in Digital Communications and Signal Processing and the Head of Institute for Digital Communications. His research interests include signal processing and information theoretic aspects of 5G and beyond wireless networks, full-duplex radio, mmWave communications, random matrices theory, interference alignment, statistical and array signal processing and quantum information theory. He has published over 325 publications in these areas and holds four U.S. patents. He was the coordinator of the FP7 projects ADEL (3.7M€) in the area of licensed shared access for 5G wireless networks and HARP (3.2M€) in the area of highly distributed MIMO and FP7 Future and Emerging Technologies projects HIATUS (2.7M€) in the area of interference alignment and CROWN (2.3M€) in the area of cognitive radio networks. Dr Ratnarajah is a Fellow of Higher Education Academy (FHEA), U.K..

Constantinos B. Papadias is the Dean of Athens Information Technology (AIT), in Athens, Greece, where he is also Professor and Head of its Broadband Wireless and Sensor Networks (B-WiSE) Research Group. He is also Adjunct Professor at Aalborg University. He received the Diploma of Electrical Engineering from the National Technical University of Athens (NTUA) in 1991 and the Doctorate degree in Signal Processing (highest honors) from the Ecole Nationale Supérieure des Télécommunications (ENST), Paris, France, in 1995. He was a researcher at Institut Eurécom (1992-1995), Stanford University (1995-1997) and Bell Labs (as Member of Technical Staff from 1997-2001 and as Technical Manager from 2001-2006). He was also Adjunct Professor at Columbia University (2004-2005) and Carnegie Mellon University (2006-2011). He has published over 180 papers and 3 books and has received over 7500 citations for his work, with an h-index of 40. He has also made standards contributions and holds 12 patents. He was a member of the Steering Board of the Wireless World Research Forum (WWRF) from 2002-2006, a member and industrial liaison of the IEEEs Signal Processing for Communications Technical Committee from 2003-2008 and a National Representative of Greece to the European Research Councils IDEAS program from 2007-2008. He has served as member of the IEEE Communications Societys Fellow Evaluation and Awards Committees, as well as an Associate Editor for various journals. He has contributed to the organization of several conferences, such as IEEE Globecom 2014 (Workshops Chair), IEEE CTW 2016 (General Chair), the IEEE ICC 2017 (Workshops Chair) and the upcoming IEEE SPAWC 2018 (General Chair). He has acted as Technical Coordinator in several EU projects such as: CROWN in the area of cognitive radio; HIATUS in the area of interference alignment; HARP in the area of remote radio heads and ADEL in the area of licensed shared access. His distinctions include the Bell Labs Presidents Award (2002), the IEEE Signal Processing Societys Young Author Best Paper Award (2003), a Bell Labs Teamwork Award (2004), his recognition as a Highly Cited Greek Scientist (2011), two IEEE conference paper awards (2013, 2014) and a Best Booth Award at EUCNC (2016). He was a Distinguished Lecturer of the IEEE Communications Society for 2012-2013 and is a Fellow of IEEE.